Received 30 January 2020; revised 14 April 2020; accepted 4 May 2020. Date of publication 11 May 2020; date of current version 7 August 2020.
The review of this article was arranged by Editor J. Knoch.

Digital Object Identifier 10.1109/JEDS.2020.2993705

Enhancement of Room-Temperature Effective Spin Diffusion Length in a Si-Based Spin MOSFET With an Inversion Channel

RYOSHO NAKANE [1] (Member, IEEE), SHOICHI SATO [2], AND MASAAKI TANAKA [3]

1 Department of Electrical Engineering and Information Systems, Institute for Innovation in International Engineering Education, University of Tokyo, Tokyo 113-8656, Japan
2 Department of Electrical Engineering and Information Systems, University of Tokyo, Tokyo 113-8656, Japan
3 Department of Electrical Engineering and Information Systems, Center for Spintronics Research Network, University of Tokyo, Tokyo 113-8656, Japan

CORRESPONDING AUTHOR: R. NAKANE (e-mail: nakane@cryst.t.u-tokyo.ac.jp)

This work was supported in part by Grants-in-Aid for Scientific Research under Grant 20H02199, Grant 16H02095 and Grant 18H05345, in part by CREST of JST under Grant JPMJCR1777, and in part by the Spintronics Research Network of Japan.

ABSTRACT We have demonstrated a Si-based bottom-gate-type spin metal-oxide-semiconductor field-effect transistor (spin MOSFET) with an electron inversion channel at room temperature and showed the enhancement of the room-temperature effective spin diffusion length by "spin drift". Our spin MOSFET was fabricated on a (001)-oriented silicon-on-insulator (SOI) substrate with a *p*-type ultrathin (8 nm) Si layer, in which the channel length was 1.0 μm, the spin injector/detector electrodes were ferromagnetic multilayer (from top to bottom) Fe(4nm)/Mg(1nm)/MgO(1nm) tunnel junctions, and a 200-nm-thick buried oxide layer was used for the gate dielectric. Using various gate electric fields and source-drain electron currents, two types of spin-dependent transport signals were measured: spin-valve signals with an in-plane magnetic field and Hanle signals with an out-of-plane magnetic field. Clear Hanle signals and spin-valve signals were obtained for various bias conditions. We analyzed the Hanle signals and the change of the spin-valve signals based on our original formulas that take into account the distribution of the lateral electric field along the electron transport, and revealed that the spin drift can enhance the effective spin diffusion length by the lateral electric field parallel to the electron transport in the inversion channel. The effective spin diffusion length becomes 3−13 times larger than the intrinsic spin diffusion length $\lambda_S = 0.89$ μm owing to the increase in the lateral electric field. It was confirmed that the spin drift is very useful to achieve larger spin-valve signals in spin MOSFETs with an electron inversion channel.

INDEX TERMS Silicon devices, spin polarized transport, spin valves.

I. INTRODUCTION

Silicon-based spin metal-oxide-semiconductor field-effect transistors (spin MOSFETs [1]–[4]) are attractive for next-generation electronics on a Si platform, since they can be key devices in nonvolatile memory as well as reconfigurable logic circuits. Lateral-type spin MOSFETs have basically the same device structure as ordinary MOSFETs, but their source/drain (S/D) electrodes are replaced with ferromagnets or ferromagnetic multilayers (FM). The spin-dependent output characteristics of spin MOSFETs result from the variable transconductance depending on the relative magnetization configuration (from parallel to antiparallel) of the S and D ferromagnets. The origin is the spin-valve effect similar to the giant magnetoresistance effect. The charge and spin transport consists of three processes; 1) injection of spin-polarized electrons at the S junction into the Si channel, 2) spin-preserving electron transport through the Si two-dimensional (2D) inversion/accumulation channel, and 3) detection of spin-polarized electrons at the D junction. In this operation principle, there are two building blocks: S/D junctions and an electron inversion/accumulation channel of Si. In the S/D junctions, higher magnetoresistance change requires spin injection and detection with higher efficiency. So far, spin injection and detection into/from a n^+-Si

channel have been extensively studied utilizing ferromagnetic multilayers, such as Fe/MgO/Si [5], Fe/Mg/MgO/Si [6], Fe/Mg/MgO/SiO_x/Si [7], and Fe/Mg/SiO_xN_y/Si [8] tunnel junctions, and there have been some guidelines to improve the performance. Particularly, our recent paper with Fe/Mg/MgO/SiO_x/Si junctions [7] achieved the maximum spin injection efficiency (~93%) by suppressing the formation of a magnetically-dead layer at the Fe/MgO interface as well as by suppressing the electron traps at the MgO/Si interface.

On the other hand, in an electron inversion/accumulation channel, higher magnetoresistance change requires longer effective spin diffusion length λ_S^{eff}. When electron transport is completely diffusive, λ_S^{eff} is equal to the intrinsic spin diffusion length λ_S, that is, $\lambda_S^{eff} = \lambda_S = (D_e\tau_S)^{0.5}$, where D_e is the electron diffusion coefficient and τ_S is the spin lifetime. In this case, λ_S is an intrinsic property that is determined by the channel material and channel structure, and longer λ_S requires longer τ_S. For this requirement, Si has a potential capability to have a long τ_S due to its small spin-orbit coupling. Theoretically, electron spin scattering in Si is dominated by the Elliot-Yafet mechanism [9] which predicts that a part of electron momentum scattering events can flip electron spins. In the demonstration of *n*-type Schottky-barrier spin MOSFETs at room temperature [4], our quantitative analyses revealed that the τ_S/τ ratio (τ is the momentum lifetime) is constant (~14000) in an electron accumulation channel of Si with a phosphorus donor doping concentration $N_D = 1 \times 10^{17}$ cm^{-3} even when the dominant scattering mechanism was changed from the phonon scattering to the surface roughness scattering by the gate electric field. Since the τ_S/τ ratio ~14000 is smaller by a factor of four than that (45000 – 77000) estimated from the ESR measurement for a bulk Si material with a similar phosphorus donor doping concentration [10], there is a possibility that the spin-orbit coupling in the electron accumulation channel is larger than that in Si bulk materials. Although spin MOSFETs with an electron inversion channel have not yet been reported, smaller τ_S/τ ratio is also anticipated. To overcome this problem, increase of the lateral electric field along the electron transport is one possible method to achieve a longer λ_S^{eff} while τ_S and τ remain unchanged [11]. This is called "spin drift". So far, the spin drift in a n^+-Si channel has been experimentally reported [12]; however, there is no report on the spin drift in an electron inversion channel.

In this study, we demonstrate bottom-gate-type spin MOSFETs with an electron inversion channel at room temperature, and then quantitatively investigate the spin drift by our experimental results and our original formulas that precisely take into account the distribution of the lateral electric field. Our results clearly show that the spin drift is very useful to enhance λ_S^{eff} even when electron momentum scatterings become much more frequent due to an ultrathin body (8 nm) Si channel.

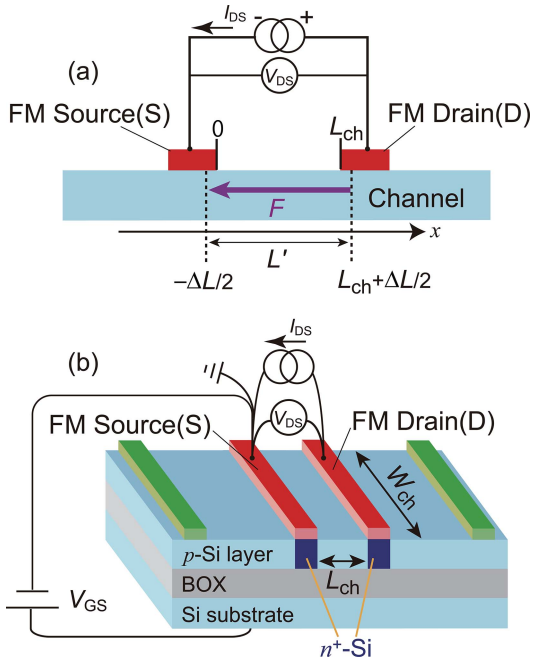

FIGURE 1. **(a) Side view of a schematic device structure and the two-terminal measurement for spin-valve signals, where S and D represent the source and drain electrodes (which are ferromagnetic multilayers (FM), see the text), respectively, the blue region is a Si channel. Here, it is assumed that electrons travel from $x = -\Delta L/2$ to $x = L_{ch} + \Delta L/2$ through the Si channel and the lateral electric field F is present along the $-x$ direction due to the application of a constant electron current I_{DS} from the S to D electrodes. In our model, F is present between $-\Delta L/2$ and $L_{ch} + \Delta L/2$. Here, L' is defined by $L_{ch} + \Delta L$. (b) Schematic illustration of our spin MOSFET fabricated on a (001)-oriented silicon-on-insulator (SOI) substrate with a buried oxide (BOX) layer having a thickness $t_{BOX} = 200$ nm, where the 3-nm-thick p-type Si layer is the channel, the spin injector/detector (denoted as Source and Drain) formed on the Si(001) surface are ferromagnetic multilayer (from top to bottom) Fe(4nm)/Mg(1nm)/MgO(1nm) tunnel junctions, and the BOX layer is the gate dielectric. The deep blue regions are n^+-Si regions formed under the S and D electrodes. The designed chanel width W_{ch} and length L_{ch} are defined in the figure. The measurement setup for spin-dependent signals is also shown: Constant source-to-drain electron current I_{DS} and source-to-gate voltage V_{GS} are applied and the source-drain voltage V_{DS} is measured while an in-plane magnetic field is applied along the longitudinal direction of the S and D electrodes or an out-of-plane magnetic field is applied. The green electrodes outside the S and D electrodes are not used in this study.**

II. THEORY OF SPIN DRIFT AND PROCEDURE OF ANALYSIS

Fig. 1(a) shows a side view of our schematic device structure and the two-terminal measurement for spin-valve signals, where S and D represent the FM source and FM drain electrodes, respectively, the blue region is a Si channel, and L_{ch} is the designed Si channel length. It is well-recognized that the designed (physical) channel length can be different from the electrical channel length where electrons are transported. Considering this possibility, it is assumed that electrons are transported from $x = -\Delta L/2$ to $L_{ch} + \Delta L/2$ through the Si channel, as defined in Fig. 1(a), meaning that the electrical channel length is $L' = L_{ch} + \Delta L$. In the channel with a length L', a lateral electric field F is present along the $-x$ direction due to the application of a constant

electron current I_{DS} from the S to D electrodes. Although the previous paper [12] assumed that a uniform F is present between $-\infty$ and ∞, actually F is present only between the S and D electrodes. Thus, our model is more realistic and practical for this measurement geometry. This difference in the F distribution leads to the different boundary conditions of the spin density at $x = -\Delta L/2$ and $L_{ch} + \Delta L/2$. Spin diffusion lengths along the $\pm x$ directions are different due to F [11]: Upstream spin diffusion length λ^{u} along the $-x$ direction and downstream spin diffusion length λ^{d} along the $+x$ direction. These are defined by

$$\Lambda = D_e/v_d, \tag{1}$$

$$\left(\lambda^{u(d)}\right)^{-1} = +(-)(2\Lambda)^{-1} + \sqrt{(2\Lambda)^{-2} + (\lambda_s)^{-2}}, \tag{2}$$

where v_d is the drift velocity of electrons, $\lambda^{u} < \lambda^{d}$, and $\lambda^{u}\lambda^{d} = (\lambda_S)^2$. When v_d is small, the spin diffusion governs the spin transport and $\lambda^{u} = \lambda^{d} = \lambda_S$. As will be shown in Section IV, $\lambda^{u} \ll \lambda^{d}$ holds under the bias conditions experimentally examined in this study. Thus, λ^{d} governs the spin transport via the Si inversion channel and it is regarded as λ_S^{eff} enhanced by the spin drift, i.e., $\lambda_S^{eff} \cong \lambda^{d}$. In our study, two types of spin-dependent transport signals via the Si inversion channel are measured and analyzed: spin-valve signals with an in-plane magnetic field $H_{//}$ and Hanle signals with an out-of-plane magnetic field $H_{\perp}$. Since V_{GS} and I_{DS} are constant in the measurement of the spin-dependent transport signals using a spin MOSFET with a channel width W_{ch}, $v_d = I_{DS}/qN_S W_{ch}$ for a certain I_{DS} can be estimated from a Hall measurement with a certain V_{GS}, where q is the elementary charge and N_S is the sheet electron density. The methods for D_e and N_S estimation will be described later. Using the v_d and D_e values, Λ is estimated by Eq. (1).

In both spin-dependent transport signals, the voltage change ΔV^{2T} between the parallel and antiparallel magnetization configurations is given by the following formula for a device with L':

$$\begin{aligned}
\Delta V^{2T}(L') &= 2V_0 A\left[B\exp\left(L'/\lambda^{d}\right) - C\exp\left(-L'/\lambda^{u}\right)\right]^{-1},\\
V_0 &= P_S^2 I_{DS} R_S \lambda_S / W_{ch}\\
A &= \left(\lambda_S/\lambda^{d}\right) + \left(\lambda_S/\lambda^{u}\right),\\
B &= \left(1 + \lambda_S/\lambda^{d}\right)\left(1 + \lambda_S/\lambda^{u}\right),\\
C &= \left(1 - \lambda_S/\lambda^{d}\right)\left(1 - \lambda_S/\lambda^{u}\right),
\end{aligned} \tag{3}$$

where P_S is the tunneling electron spin polarization and R_S is the sheet resistance of the Si inversion channel. On the other hand, the Hanle signal is expressed by introducing the complex spin diffusion lengths $\widehat{\lambda}_s$, $\widehat{\lambda}^{u}$, and $\widehat{\lambda}^{d}$ [6]:

$$\widehat{\lambda}_s = \lambda_s(1 + i\gamma H_\perp \tau_s)^{\frac{1}{2}},$$

$$\left(\widehat{\lambda}^{u(d)}\right)^{-1} = +(-)(2\Lambda)^{-1} + \sqrt{(2\Lambda)^{-2} + \left(\widehat{\lambda}_s\right)^{-2}},$$

$$\Delta V^{2TH,\,P(AP)}(H_\perp) = -(+)\mathrm{Re}\left[V_0 A\left[B\exp\left(L'/\widehat{\lambda}^{d}\right) - C\exp\left(-L'/\widehat{\lambda}^{u}\right)\right]^{-1}\right], \tag{4}$$

where i is the imaginary unit, Re[] means the real part of the complex number in the parentheses, $\gamma = 1.76 \times 10^{11}$ rad/Ts is the gyromagnetic ratio, P and AP denote the parallel and antiparallel magnetization configurations, respectively, and $\Delta V^{2TH,P}(H_\perp)$ and $\Delta V^{2TH,AP}(H_\perp)$ are Hanle signals measured for P and AP, respectively. Note that $(\Delta V^{2TH,AP} - \Delta V^{2TH,P})$ is the maximum value at $H_\perp = 0$, which corresponds to ΔV^{2T} in Eq. (3).

P_S, τ_S, and ΔL are estimated at the same time by fitting Eq. (4) to Hanle signals measured with three I_{DS} values and a constant V_{GS}, under the condition that P_S, τ_S ($=\lambda_S^2/D_e$), and ΔL have the same values for the same V_{GS}. Then, assuming that the ΔL and τ_S values are the same for all V_{GS}, P_S is estimated by fitting Eq. (3) to ΔV^{2T} obtained from spin-valve signals measured with various I_{DS} and V_{GS}. Finally, λ_S^{eff} ($\cong \lambda^{d}$) and λ^{u} are estimated for each bias condition (V_{GS} and I_{DS}) and they are compared with λ_S to reveal the enhancement due to the spin drift.

III. DEVICE STRUCTURE AND MEASUREMENT SETUP

Fig. 1(b) shows a schematic view of a bottom-gate-type spin MOSFET fabricated on a (001)-oriented silicon-on-insulator (SOI) substrate with a buried oxide (BOX) layer having a thickness $t_{BOX} = 200$ nm, where the spin injector/detector (referred to as the S/D electrodes) formed on the Si(001) surface are ferromagnetic multilayer (from top to bottom) Fe(4nm)/Mg(1nm)/MgO(1nm) tunnel junctions and the BOX layer was used for the gate dielectric. The fabrication process and device structure were basically the same as those in our previous paper [4]. Here, the main differences and device parameters are described below. For the MOSFETs with an electron inversion channel, a 8-nm-thick Si channel layer has a boron acceptor doping concentration $N_A = 10^{15}$ cm^{-3} and phosphorous-doped Si regions with $N_D \sim 10^{20}$ cm^{-3} (denoted by n^+-Si in the figure) were formed under the S/D electrodes using a spin-coated phosphorus glass and thermal diffusion. The designed channel width W_{ch} and length L_{ch} were 180 and 1.0 μm, respectively. The width and length of the S electrode were 0.7 and ~180 μm, respectively, and those of the D electrode were 2 and ~180 μm, respectively. In the measurement of spin-dependent transport signals at 295 K, a constant gate-source voltage V_{GS} and a constant electron current I_{DS} were applied and the source-drain voltage V_{DS} was measured. For spin-valve signals, $H_{//}$ was applied along the longitudinal direction of the S/D electrodes. Four different sweeping sequences were used for $H_{//}$;

(A) Major loop of the spin-valve signal: $H_{//}$ was swept between ±8 kA/m.
(B) Minor loop of the spin-valve signal: $H_{//}$ was swept from +8 kA/m to −5.1 kA/m and then swept back to +8 kA/m.

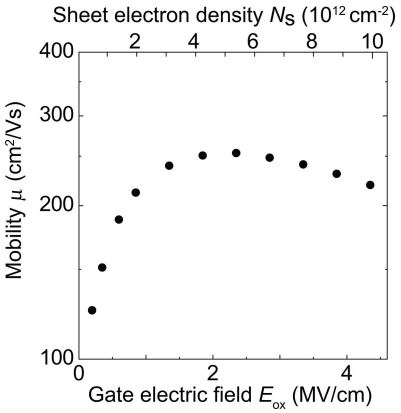

FIGURE 2. **Low-field electron mobility μ at 295 K plotted as a function of gate electric field E_{OX}, which were estimated from a Hall-bar-type MOSFET fabricated on the same substrate. The sheet electron density N_S is also shown in the upper axis.**

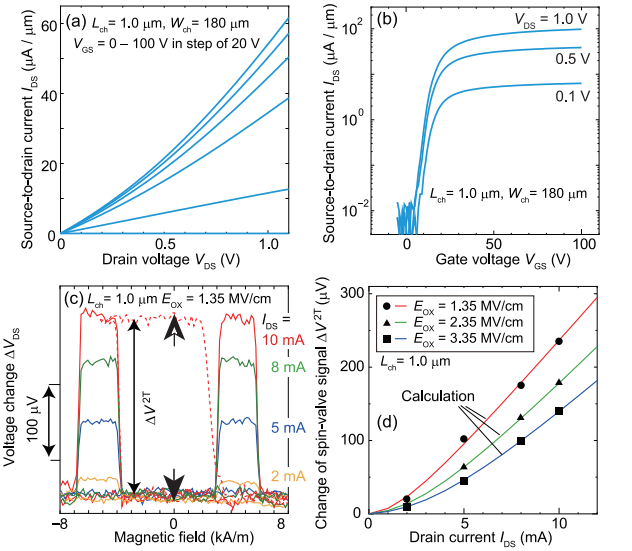

FIGURE 3. **(a) I_{DS}-V_{DS} and (b) I_{DS}-V_{GS} characteristics at 295 K of a spin MOSFET with L_{ch} = 1.0μm. In (a), V_{GS} is varied from 0 to 100 V in step of 20 V. (c) Spin-valve signals at 295 K measured with E_{OX} = 1.35 MV/cm (V_{GS} = 40 V) for the spin MOSFET with L_{ch} = 1.0μm as a function of in-plane magnetic field $H_{//}$, where colored solid and dotted curves are major and minor loops, respectively, and I_{DS} for each major loop is denoted. The change of the spin-valve signal ΔV^{2T} is defined for the case of I_{DS} = 10 mA. The closed and open arrows at $H_{//}$ = 0 denote the ΔV_{DS} values for P and AP, respectively. (d) ΔV^{2T} plotted as a function of I_{DS}, which were estimated from the spin-valve signals measured at 295 K with I_{DS} (= 2, 5, 8, and 10 mA) and E_{OX} (= 1.35, 2.35, and 3.35 MV/cm) for the spin MOSFET with L_{ch} = 1.0μm. The black circles, triangles, and squares are experimental values for E_{OX} = 1.35, 2.35, and 3.35 MV/cm, respectively, and the red, green, and blue curves denoted by "Calculation" are the fitting curves by Eq. (3) for E_{OX} = 1.35, 2.35, and 3.35 MV/cm, respectively.**

(C) Initialization for Hanle signals with P: $H_{//}$ was swept from +8 to 0 kA/m.

(D) Initialization for Hanle signals with AP: $H_{//}$ was swept from +8 to −5.1 kA/m and then swept back to 0 kA/m.

For Hanle signals, $H_{\perp}$ was swept between ±160 kA/m or between ±80 kA/m after the initialization by the sweeping sequence (C) or (D). Hereafter, the gate electric field $E_{OX} = (V_{GS} - V_{TH})/t_{BOX}$ is mainly used, where V_{TH} = 13 V is the threshold voltage estimated from N_S.

To estimate N_S and the low-field effective electron mobility μ in an electron inversion channel at E_{OX} (= 0.35 − 4.35 MV/cm), a Hall-bar-type MOSFET was also prepared on the same substrate. Using the Hall voltage and sheet resistance at 295 K, N_S and μ were estimated under an assumption that the Hall factor is equal to 1 [13]. To estimate F in the bias conditions of spin-dependent transport signals, $F = R_S I_{DS}/W_{ch}$ is used.

IV. EXPERIMENTAL RESULTS

A. HALL-BAR-TYPE MOSFET

Fig. 2 shows μ plotted as a function of E_{OX}. The μ values are significantly smaller than the universal mobility [14], probably because of the increase in electron scatterings originating from the ultrathin channel layer 8 nm [13], [15]. Owing to the difficulty in the estimation of D_e in such an ultrathin Si channel layer by a self-consistent calculation, D_e was calculated from μ estimated for a 15-nm-thick Si channel layer in our previous paper [4], assuming that D_e is proportional to μ.

B. SPIN MOSFETS

Figs. 3(a) and (b) show I_{DS}-V_{DS} and I_{DS}-V_{GS} characteristics, respectively, which demonstrate a clear transistor operation. In Fig. 3(a), the slight downward bend of I_{DS} in higher V_{DS} and V_{GS} mainly originates from the parasitic resistance of the Fe/Mg/MgO/n^+-Si(001) tunnel junctions at the S/D electrodes.

Fig. 3(c) shows ΔV_{DS} signals measured with $H_{//}$, E_{OX} = 1.35 MV/cm (V_{GS} = 40 V), and various I_{DS} (= 2, 5, 8, and 10 mA), where solid curves represent major loops and a broken curve is a minor loop measured with I_{DS} = 10 mA. From both major and minor loops, the hysteretic signal change results from the change in the magnetization configurations (P/AP), i.e., the spin-valve signal. Thus, Figs. 3(a), (b), and (c) demonstrate the spin MOSFET operation with an electron inversion channel. In Fig. 3(c), the change of the spin-valve signal ΔV^{2T} is defined for the case of I_{DS} = 10 mA. The maximum magnetoresistance ratio obtained for I_{DS} = 10 mA is 0.018% that was estimated by $\Delta V^{2T}/V_{DS}$ at $H_{\perp}$ = 0.

In the same manner, spin-valve signals were also measured with various E_{OX} (= 2.35 and 3.35 MV/cm) and I_{DS} (= 2, 5, 8, 10 mA) and these ΔV^{2T} values were plotted as a function of I_{DS} for each V_{GS}. Fig. 3(d) shows ΔV^{2T} plotted as a function of I_{DS}, where black circles, triangles, and squares are experimental values for E_{OX} = 1.35, 2.35, and 3.35 MV/cm, respectively. At the same E_{OX}, the non-linear increase in the experimental ΔV^{2T} value with increasing I_{DS} (increasing F) indicates that the spin drift was developed in our spin MOSFET, since a linear increase would be obtained if λ_S^{eff} were unchanged with increasing F.

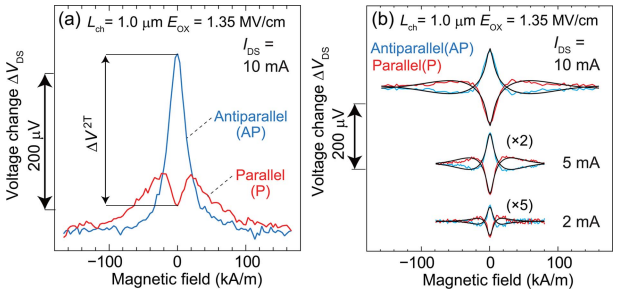

FIGURE 4. (a) ΔV_{DS} signals measured at 295 K with E_{OX} = 1.35 MV/cm (V_{GS} = 40 V) and I_{DS} = 10 mA, as a function of out-of-plane magnetic field $H_\perp$ for the spin MOSFET with L_{ch} = 1.0μm, where red and blue curves are the signals with the P and AP magnetization configurations, respectively, and ΔV^{2T} at $H_\perp$ = 0 is indicated. (b) Hanle signals at 295 K estimated from the ΔV_{DS} signals shown in (a) measured with E_{OX} = 1.35 MV/cm (V_{GS} = 40 V) and I_{DS} = 2, 5, and 10 mA, where red and blue curves are the Hanle signals with the parallel (P) and antiparallel (AP) magnetization configurations, respectively. The Hanle signals for 2 and 5 mA are multiplied by 5 and 2, respectively, and black curves are the fitting curves by Eq. (4).

In Fig. 3(c), closed and open arrows at $H_{//} = 0$ denote the ΔV_{DS} values for P and AP, respectively, which can be realized by the sweeping sequences (C) and (D), respectively. Using these P and AP as the initial states, out-of-plane signals were measured with $E_{OX} = 1.35$ MV/cm ($V_{GS} = 40$ V) and various I_{DS} (= 2, 5, and 10 mA) while $H_\perp$ was swept. Fig. 4(a) show out-of-plane signals measured with $I_{DS} = 10$ mA, where red and blue curves represent the signals for P and AP, respectively. The difference in ΔV_{DS} at $H_\perp = 0$ is 235 μV that agrees well with the ΔV^{2T} value for $I_{DS} = 10$ mA in Fig. 3(c). Based on the theory in our previous paper [4], we found that the out-of-plane signals in Fig. 4(a) contain signals originating from various phenomena and the Hanle signal due to the spin transport via the Si inversion channel can be extracted by subtraction: the Hanle signal with P (AP) is obtained by the half of P − AP (AP − P) in Fig. 4(a). Fig. 4(b) shows Hanle signals for $E_{OX} = 1.35$ MV/cm ($V_{GS} = 40$ V) and $I_{DS} = 2, 5,$ and 10 mA, where red and blue curves represent the experimental Hanle signals with P and AP, respectively, and black curves are the fitting curves by Eq. (4). In the Hanle signal, the oscillation and decaying amplitude originate from the spin precession (phase change of spin) and spin dephasing due to the spin diffusion, respectively, during the transport from the S to D electrodes via the Si inversion channel. In the oscillation, the half of the $H_\perp$ period that is $\Delta H_\perp$ for the nearest two peaks corresponds to π phase change during the transport and it is expressed by $(\Delta H_\perp)_\pi \cong (v_d\pi)/(\gamma\mu_0 L')$, where μ_0 is the vacuum permeability. Thus, $(\Delta H_\perp)_\pi$ increases with increasing I_{DS} ($\propto v_d$). In Fig. 4(b), such trend is clearly seen: The oscillation period increases with increasing I_{DS}. This indicates the spin drift. In fact, the fitting curves (black curves), which take into account the spin drift, well reproduce the experimental signals (red and blue curves) in Fig. 4(b). Furthermore, although the signals with $I_{DS} = 2$ and 5 mA are multiplied by 5 and 2, respectively, the ΔV^{2T} values (the signal amplitudes at $H_\perp = 0$) are different and the order of the amplitude is $10 > 5 > 2$ mA. This result also indicates the spin drift, since the same amplitudes would be obtained if the amplitude is determined only by I_{DS}. From the fittings, $P_S = 1.9\%$, $\tau_S = 0.94$ ns, and $\Delta L = 0.5$ μm were obtained. Using $D_e = 8.4$ cm^2/s estimated from the Hall-bar-type device with $E_{OX} = 1.35$ MV/cm, $\lambda_S = 0.89$ μm was obtained. This value is consistent with that ($\lambda_S = 0.80-0.95$ μm) obtained for our Schottky-barrier spin MOSFETs with a lightly-phosphorus-doped accumulation channel [4]. Thus, the channel type (inversion or accumulation) was found to have little influence on λ_S.

Using these τ_S and ΔL values, ΔV^{2T} in Fig. 3(d) were fitted by Eq. (3) with the free parameter P_S, where red, green, and blue curves denoted by "Calculation" are the fitting curves for $E_{OX} = 1.35, 2.35$ and 3.35 MV/cm, respectively. The good agreement between the experimental values and fitting curves confirms that our theory can accurately analyze the spin drift. From all our analyses, the following values were obtained for $E_{OX} = 1.35$ MV/cm: $\lambda_S = 0.89$ μm, $\lambda_S^{eff} \cong \lambda^d = 3.08$ μm, and $\lambda^u = 0.31$ μm for $I_{DS} = 2$ mA ($|F| = 0.94$ kV/cm), $\lambda_S^{eff} \cong \lambda^d = 7.05$ μm, and $\lambda^u = 0.14$ μm for $I_{DS} = 5$ mA ($|F| = 2.36$ kV/cm), and $\lambda_S^{eff} \cong \lambda^d = 13.89$ μm, and $\lambda^u = 0.07$ μm for $I_{DS} = 10$ mA ($|F| = 4.71$ kV/cm). Clearly, the λ_S^{eff} values are 3−13 times larger than the intrinsic $\lambda_S = 0.89$ μm. Thus, the spin drift was confirmed in our spin MOSFET with an electron inversion channel.

It should be noted that our experimental ΔV^{2T}-I_{DS} plot in Fig. 3(d) could not be fitted by Eq. (3) in [12]. This comes from the fact that the distribution of F in their model does not reflect the real condition. Thus, our model taking into account the distribution of F along the electron transport is valid to analyze the spin drift in lateral-type spin transport devices with the two-terminal measurement geometry in Fig. 1(a).

V. CONCLUSION

We have demonstrated Si-based bottom-gate-type spin MOSFET with an electron inversion channel at room temperature and have clarified the spin drift effect in the channel based on our original formulas. The experimental Hanle signals and ΔV^{2T} estimated from the spin-valve signals measured with various I_{DS} and E_{OX} were well fitted by the formulas, which means that our analysis is valid. The λ_S^{eff} values are larger by a factor of 3−13 than the intrinsic $\lambda_S = 0.89$ μm, which confirms that the spin drift is very useful to obtain a larger magnetoresistance ratio in spin MOSFETs with an electron inversion channel.

The maximum magnetoresistance ratio 0.018% is not enough for practical use. This small value comes from various origins. One is the ultrathin p-type Si channel layer that significantly enhances electron momentum scattering due to acoustic phonons. Considering the experimental investigations reported in the past, when a lightly-doped n-type thicker

Si channel layer in a SOI substrate is used, the magnetoresistance ratio is expected to be larger owing to the reduction in electron momentum scatterings. Indeed more extensive studies are indispensable to advance the technology of spin MOSFETs, but the results obtained in this study serve as an important step for the appropriate design of spin MOSFETs.

ACKNOWLEDGMENT

The authors thank M. Ichihara (The University of Tokyo) for his help in the device fabrication.

REFERENCES

[1] S. Sugahara and M. Tanaka, "A spin metal–oxide–semiconductor field-effect transistor using half-metallic-ferromagnet contacts for the source and drain," *Appl. Phys. Lett.*, vol. 84, pp. 2307–2309, Jan. 2004.
[2] M. Tanaka and S. Sugahara, "MOS-based spin devices for reconfigurable logic," *IEEE Trans. Electron Devices*, vol. 54, no. 5, pp. 961–976, May 2007.
[3] T. Tahara *et al.*, "Room-temperature operation of Si spin MOSFET with high on/off spin signal ratio," *Appl. Phys. Exp.*, vol. 8, pp. 1–3, Oct. 2015.
[4] S. Sato, M. Ichihara, M. Tanaka, and R. Nakane, "Electron spin and momentum lifetimes in two-dimensional Si accumulation channels: Demonstration of Schottky-barrier spin metal-oxide-semiconductor field-effect transistors at room temperature," *Phys. Rev. B*, vol. 99, pp. 1–9, Apr. 2019.
[5] T. Suzuki, T. Sasaki, T. Oikawa, M. Shiraishi, Y. Suzuki, and K. Noguchi, "Room-temperature electron spin transport in a highly doped Si channel," *Appl. Phys. Exp.*, vol. 4, pp. 1–3, Feb. 2011.
[6] S. Sato, R. Nakane, T. Hada, and M. Tanaka, "Spin injection into silicon in three-terminal vertical and four-terminal lateral devices with Fe/Mg/MgO/Si tunnel junctions having an ultrathin Mg insertion layer," *Phys. Rev. B*, vol. 96, pp. 1–10, Dec. 2017.
[7] R. Nakane, M. Ichihara, S. Sato, and M. Tanaka, "Nearly ideal spin tunneling efficiency in Fe/Mg/MgO/SiO_x/n^+-Si(001) junctions," *Phys. Rev. Mater.*, vol. 3, pp. 1–9, Feb. 2019.
[8] R. Nakane, T. Hada, S. Sato, and M. Tanaka, "Spin transport and spin accumulation signals in Si studied in tunnel junctions with a Fe/Mg ferromagnetic multilayer and an amorphous Si_xN_y tunnel barrier," *Appl. Phys. Lett.*, vol. 112, no. 18, pp. 1–4, Apr. 2018.
[9] R. J. Elliott, "Theory of the effect of spin-orbit coupling on magnetic resonance in some semiconductors," *Phys. Rev.*, vol. 96, no. 2, pp. 266–279, Oct. 1954.
[10] I. Gränacher and W. Czaja,"Mobility and electron spin resonance linewidth in phosphorus doped silicon," *J. Phys. Chem. Solids*, vol. 28, no. 2, pp. 231–238, Feb. 1967.
[11] Z. G. Yu and M. E. Flatté, "Spin diffusion and injection in semiconductor structures: Electric field effects," *Phys. Rev. B*, vol. 66, pp. 1–14, Dec. 2002.
[12] M. Kameno *et al.*, "Spin drift in highly doped n-type Si," *Appl. Phys. Lett.*, vol. 104, no. 9, pp. 1–4, Feb. 2014.
[13] S. Kobayashi, M. Saitoh, Y. Nakabayshi, T. Ishihara, T. Numata, and K. Uchida, "Hall factor in ultrathin-body silicon-on-insulator n-type metal–oxide–semiconductor field-effect transistors," *Jpn. J. Appl. Phys.*, vol. 49, pp. 1–5, Apl. 2010.
[14] S. Takagi, A. Toriumi, M. Iwase, and H. Tango, "On the universality of inversion layer mobility in Si MOSFET's: Part I-effects of substrate impurity concentration," *IEEE Trans. Electron Devices*, vol. 41, no. 12, pp. 2357–2362, Dec. 1994.
[15] T. Ohashi, T. Tanaka, T. Takahashi, S. Oda, and K. Uchida, "Experimental study on deformation potential (Dac) in MOSFETs: Demonstration of increased Dac at MOS interfaces and its impact on electron mobility," *IEEE J. Electron Devices Soc.*, vol. 4, no. 5, pp. 278–285, Sep. 2016.

RYOSHO NAKANE (Member, IEEE) received the B.S. and M.S. degrees in electronic engineering from Hokkaido University, Sapporo, Japan, in 2000 and 2002, respectively, and the Ph.D. degree in electronic engineering from the University of Tokyo, Tokyo, Japan, in 2005.

Since 2013, he has been a Project Research Associate Professor with the University of Tokyo. His current research interests include semiconductor-based spintronic devices, semiconductor-based electronic devices for next-generation integrated circuits, and machine-learning electronic devices for energy-efficient information processing.

Dr. Nakane is a member of the IEEE Electron Device Society and the Japan Society of Applied Physics.

SHOICHI SATO received the B.S, M.S., and Ph.D. degrees in electronic engineering from the University of Tokyo, Tokyo, Japan, in 2009, 2011, and 2019, respectively.

Since 2019, he has been a Research Fellow with the University of Tokyo. His main interests include electrical spin injection, spin transport, and spin dynamics in semiconductors.

Dr. Sato is a member of the Japan Society of Applied Physics.

MASAAKI TANAKA received the B.E., M.E., and Ph.D. degrees in electronic engineering from the University of Tokyo, Japan, in 1984, 1986, and 1989, respectively.

He has been studying various materials, spin-related phenomena, and devices including magnetic semiconductors, ferromagnet/semiconductor heterostructures and nanostructures, magnetic tunnel junctions, and spin transistors. He is currently a Professor of electrical and electronic engineering and the Director of the Center for Spintronics Research Network, University of Tokyo. He has authored and coauthored over 280 scientific publications, and presented over 150 invited talks at international conferences and meetings.

Prof. Tanaka is a fellow of the Japan Society of Applied Physics, a member of the Physical Society of Japan and the Magnetics Society of Japan, and the Leader of the Spintronics Research Network of Japan.